Fabrication and nuclear analysis of isotopic 14N and 15N ion implanted silicon standards

Yedji, Mourad; Bolduc, Martin; Genard, Gilles; Terwagne, Guy; Ross, Guy G.

Published in:
Nuclear instruments and methods in physics research B

Publication date:
2008

Document Version
Early version, also known as pre-print

Available online at www.sciencedirect.com
ScienceDirect
Nuclear Instruments and Methods in Physics Research B 266 (2008) 2060–2064
NIM B
Beam Interactions with Materials & Atoms
www.elsevier.com/locate/nimb

Fabrication and nuclear analysis of isotopic ^{14}N and ^{15}N ion-implanted silicon standards

M. Yedji [a], M. Bolduc [a], G. Genard [b], G. Terwagne [b], G.G. Ross [a,*]

[a] INRS-Énergie, Matériaux et Télécommunications, 1650 Boulevard Lionel-Boulet, Varennes, Québec, Canada J3X 1S2
[b] Laboratoire d'Analyses par Réactions Nucléaires, FUNDP – University of Namur, 61 Rue de Bruxelles, B-5000 Namur, Belgium

Received 13 March 2008; received in revised form 18 March 2008
Available online 31 March 2008

Abstract

The fabrication of reliable isotopic nitrogen standards is achieved in Si through ^{14}N and ^{15}N ion implantation. 60 keV $^{14}N_2^+$ and $^{15}N_2^+$ ions were implanted at 400 °C up to ~60% peak atomic concentration, yielding nitrogen-saturated silicon layers as measured using resonant nuclear reaction analysis. No isotopic effect has been observed. The nitrogen standards are validated by measurements of stability under ion irradiation. No significant desorption of nitrogen is observed either under a $^4He^+$ ion fluence of 3.36×10^{16} cm^{-2} or under a $^1H^+$ ion fluence of 8.60×10^{17} cm^{-2}, giving strong evidence that isotopic nitrogen standards can be achieved.

PACS: 61.72.Tt; 35.40.Ny; 68.55.Ln; 61.80.Jh

Keywords: Ion implantation; Resonant nuclear reaction analysis; Isotopic standards; Silicon nitrides; Ion induced desorption

1. Introduction

Recent developments in the synthesis of confined and nanostructured materials have involved the use of very sensitive characterization techniques. Resonant nuclear reaction analysis (RNRA) has been recognized as a successful method for the detection of light and/or isotope elements through reaction cross-sections. This technique is attractive since it allows depth profiling and interface analysis, providing non destructive and highly quantitative measurements. For example, hydrogen detection is essential to enable further advancement on multiple applications in nanotechnology and astrophysics, such as the modification of metallic thin-films [1], the fabrication of nanoelectronic components [2–5] and silicon nanocrystals for integrated optoelectronics [6] and the understanding of nuclear reaction rates in stellar nucleosynthesis [7]. Nitrogen also plays an important role in materials engineering, especially in understanding fundamental properties of nanomaterials [8,9]. For example, the nuclear reactions $^{14}N(^3He,p)^{16}O$ and $^{14}N(^3He,\alpha)^{13}N$ have been utilized in the profiling of nitrogen in steel [10]. In addition, there is an astrophysical interest in the knowledge of reaction cross-sections under the Coulomb barrier involving, for instance, nitrogen isotopes (^{14}N and ^{15}N). The CNO cycle, first described by Hans Bethe [11], dominates the energy production for stars heavier than two solar masses and is mainly composed of four reactions where a proton is consumed: $^{12}C(p,\gamma)^{13}N$, $^{13}C(p,\gamma)^{14}N$, $^{14}N(p,\gamma)^{15}O$, and $^{15}N(p,\alpha\gamma)^{12}C$. The $^{14}N(p,\gamma)^{15}O$ reaction has been widely studied, most notably in the detection of outgoing gamma rays from irradiated ^{14}N targets [12–15]. There are many technical advantages of working with a thin target containing ^{14}N or ^{15}N ions compared to a gaseous target. A solid implanted target is more geometrically compact and may contain more than a traditional and bulky gaseous target [15].

The precise measurement of nuclear cross-section requires the use of stable and reliable reference standards of known concentration of the element on which the reaction of interest is produced. Ideally, a standard should exhibit a

* Corresponding author. Tel.: +1 450 929 8108; fax: +1 450 929 8102.
E-mail address: ross@emt.inrs.ca (G.G. Ross).

0168-583X/$ - see front matter © 2008 Elsevier B.V. All rights reserved.
doi:10.1016/j.nimb.2008.03.212

flat and thin saturated concentration profile, starting from the very near surface region (i.e. a few tenth of nanometers), while having a high degree of reproducibility. The stability of the standard under ion irradiation is a very important aspect in order to avoid desorption of the elements during non-destructive analysis. Somewhat surprisingly, to our knowledge, the fabrication of isotopic nitrogen standards via ion implantation has not been reported yet. It is thought that compounds of silicon nitrides (Si_3N_4) may have the required properties for achieving standards due to the strong binding of nitrogen atoms to silicon atoms in the lattice structure. Although Si_3N_4 thin-film materials can be fabricated by PECVD, the stoichiometry depends upon the deposition conditions [16,17]. One should note that existing nitrogen standards contain the natural isotopic abundance of nitrogen (99.634% of ^{14}N and 0.366% of ^{15}N), which is not ideal for a standard. Fortunately, ion implantation has the ability to perform standard fabrication with different isotopic elements as compared to high-cost isotopic gas in PECVD methods. Moreover, ion implantation allows the production of standard samples containing very high ^{15}N or ^{14}N isotope concentrations (close to 100%).

Nitrogen implantation in silicon has been investigated by different research groups and the results reported in literature (see for instance [18–24]). The motivation of most of these works was to create an insulating Si_3N_4 buried layer into Si wafers for microelectronic applications and, therefore, the samples were annealed at high temperature (~1200 °C) after nitrogen implantation [19–24]. Thus, the microstructure of implanted samples was characterized in order to study the damage induced by the implantation and the recovery following sample annealing. SIMS depth-profiling of N ions implanted in Si was reported [23,24]. These measurements combined to TEM characterization indicated the formation of nitrogen gas bubbles for ion fluences exceeding 1.4×10^{18} cm^{-2} with an implantation energy of 200 keV/atom [24]. However, to our knowledge, only Miyagawa et al. [20] has reported a *quantitative* depth profiling of nitrogen implanted in silicon. In their work, they also used a dynamic software that simulates the nitrogen depth profile. Calculations indicate that three different implantation energies can produce a flat profile with the Si_3N_4 stoichiometry. But the procedure (molecular or atomic ions, temperature, sequence of the implantations) is not so clear. Also, there has been no study of the retained dose as a function of the nitrogen fluence and no indication concerning the influence of the isotopic species (^{14}N or ^{15}N) on the retained dose for different implantation fluences. More, they did not report on the stability of the implanted samples under irradiation. Reproducible and reliable nitrogen depth-profiles and nitrogen stability under irradiation are two key parameters in the production of standards and are of great importance for our applications. For example, in the synthesis of photoluminescent Si-nanocrystals in SiO_2, the use of isotope ^{15}N and the resonant $^{15}N(p,\alpha\gamma)^{12}C$ nuclear reaction may permit to distinguish between the role played by the implanted nitrogen (for instance ^{15}N) and the nitrogen trapped during annealing (^{14}N) [23–25].

In this paper, we report on the fabrication and characterization of nitrogen standards in $^{14}N_2^+$ and $^{15}N_2^+$ ion implanted silicon wafers with a simple and reproducible procedure. A single energy implantation was carried out at high temperature and high fluence to allow redistribution of introduced atoms in excess of the solubility limit. The need for stable and reliable isotopic nitrogen standards is then required for precise measurements of nitrogen composition through nuclear cross-section measurements. High purity silicon nitride compounds of ^{14}N and ^{15}N having high stability under ion irradiation may indicate the synthesis of potentially new nitrogen standards in Si samples. Our experiments can also give some insights on a possible isotopic effect on the retained dose. Simulation by means of SRIM-2006 [26] indicates that although the ion depth profiles are very similar for both isotopes (because their respective velocities are close), the sputtering yield of Si is somewhat larger with the ^{15}N isotope. For instance, according to SRIM-2006, with an ion energy of 30 keV/atom, the sputtering yields are 0.84 and 0.88 for ^{14}N and ^{15}N, respectively, while the values for ion range, straggle, skewness and kurtosis are 83.7 nm, 32.7 nm, 0.16 and 0.63 for ^{14}N and 84.6 nm, 32.5 nm, 13.7 and −93.5 for ^{15}N. Simulations suggest that a larger N concentration could be obtained with the ^{14}N isotope.

2. Experimental

The $^{14}N_2^+$ and $^{15}N_2^+$ ion implanted Si samples were prepared from commercially purchased single crystal Si(1 0 0) wafers with an electronic grade surface finish. They were first cleaned in diluted HF for 5 min to remove the native oxide on the surface prior to implantation. The ion implantation was performed by means of two ion implanters equipped with magnetic mass selection stages. In the first experiment, the $^{14}N_2^+$ ions extracted from a Freeman source were implanted at an energy of 60 keV with a uniform large-area beam scanning. In the second set of experiments, the $^{15}N_2^+$ ion implantations were performed using an RF ion source mounted on a SAMES 150 kV accelerator. The extracted 60 keV $^{15}N_2^+$ beam were uniformly scanned in both axes through the application of triangular shape electric fields. Both sets of implantation were performed at room temperature but we have estimated that the incoming ion impact (~3.5 μA/cm^2) has raised the surface temperature to a maximum of ~200 °C.

First, specimens were implanted with fluences in the range (1–106) $\times 10^{16}$ atoms/cm^2 in order to obtain the saturation dose. Then, we implanted other samples to a dose of 1.06×10^{18} atoms/cm^2 at ~400 °C to promote a broad and nearly homogeneous distribution of the implanted nitrogen thanks to thermal diffusion of nitrogen atoms present in excess in the layer. Finally, it is worth mentioning that both implanters allow very good mass separation and fluence control.

The implanted nitrogen profiles were measured using resonant nuclear reaction analysis (RNRA), namely the most used $^{14}N(\alpha,\gamma)^{18}F$ and $^{15}N(p,\alpha\gamma)^{12}C$ nuclear reaction showing resonances at 1.531 MeV [27] and 0.429 MeV [28], respectively. Both reactions were extensively studied in a previous work [29]. The advantage of RNRA is the narrow and intense resonance exhibited by the cross-section leading, to an excellent depth resolution of the nitrogen profiles [7,29,31]. The reported values for the $^{15}N(p,\alpha\gamma)^{12}C$ resonances are 0.12 keV [28] and 1.56 b [30] for the width and the cross section, respectively. Concerning the $^{14}N(\alpha,\gamma)^{18}F$ resonance, Gossett mentions a width of 0.6 keV [27] and we deduce from this value and the resonance strength of 2.6 eV [32] a resonant cross section of 3.1 mb. All RNRA measurements were done with the ALTAÏS[1], the linear accelerator installed at LARN. It is a tandetron with 2 MV terminal high voltage, which allows acceleration of nearly all negative ions produced either through a source of negative ions by cesium sputtering (SNICS) or by a duoplasmatron gas source. The experimental set-up is described in more details elsewhere [7]. The ^{14}N and ^{15}N depth profiles are measured by varying step by step the incident $^4He^+$ and proton energy, so that the resonant cross section acts as a probe in the implanted nitrogen depth distribution. At each energy, gamma rays of 4.44 MeV produced by de-excitation of the ^{12}C nuclei for the ^{15}N profile and gamma rays in the range of 3.06–5.60 MeV produced by de-excitation of the ^{18}F nuclei for the ^{14}N profile were counted in a NaI(Tl) well detector.

The stability of standards is a main issue since compounds composition may change under an analyzing beam. The RNRA technique was then used as a probe to study the nitrogen depletion from the implanted layer in standards. The stability of ^{14}N and ^{15}N standards under ion beam was performed with a 200 nA beam current of 1.546 MeV $^4He^+$ ions and 250 nA beam current of 0.435 MeV $^1H^+$ ions, respectively. The total integrated charge was obtained with a Faraday cup placed in the well detector. The beam shape was circular with a diameter of 1 mm and 4 mm for $^1H^+$ and $^4He^+$ beams, respectively. Then, the total ion fluences (3.36×10^{16} $^4He^+/cm^2$ and 8.60×10^{17} $^1H^+/cm^2$) were calculated using the integrated ion charge of incident particles and the ion beam diameter. The acquisition software used in these measurements allows the counting of emitted gamma rays for a given charge range, continuously during data collection. Thus, any nitrogen desorption could be observed.

3. Results and discussion

Fig. 1 shows some depth profiles of the first set of implantations. It is visible that for high fluences the concentration exceeds Si_3N_4 composition, as predicted in [20]. Ions ranges and straggles for these depth profiles are given in Table 1. Both ion range and straggle increase with the ion fluence. Thus, it seems that the ion induced damage, which profile is nearer to the surface than the ion depth profile (according to SRIM-2006 simulation), does not promote ion trapping. The Fig. 2 shows the retained implanted

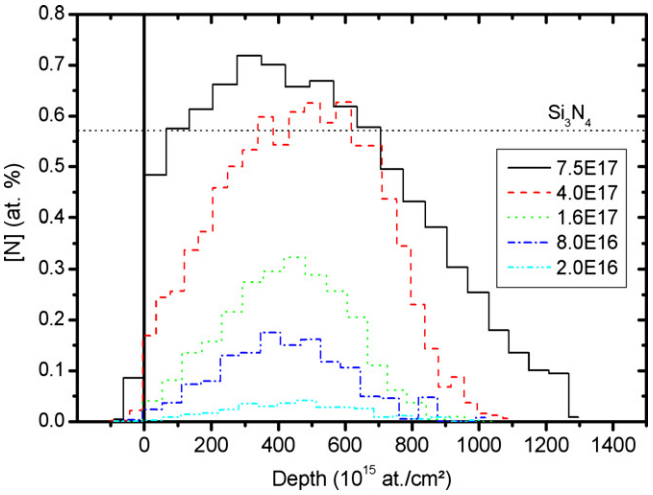

Fig. 1. Nitrogen depth profiles of some samples implanted in silicon with 60 keV N_2^+ at different fluences. The nitrogen concentration in Si_3N_4 compounds is shown.

Table 1
Ion range and straggle of the N depth profiles shown in Fig. 1

Fluence (atoms/cm²)	2.0×10^{16}	8.0×10^{16}	1.6×10^{17}	4.0×10^{17}	7.5×10^{17}
Ion range (nm)	90.3	84.1	84.5	92.0	100.8
Straggle (nm)	40.0	38.8	36.9	46.1	62.4

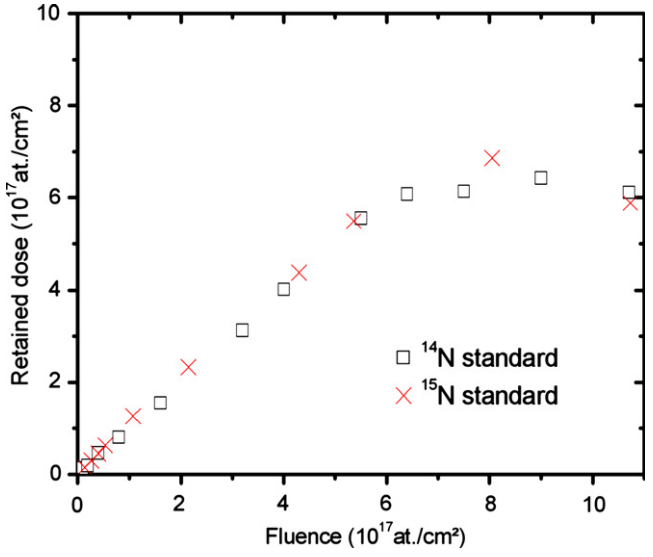

Fig. 2. Retained dose of ^{14}N and ^{15}N standards as a function of the incident nitrogen fluence. These values were obtained by integrating all nitrogen depth profiles.

[1] Accélérateur Linéaire Tandetron pour l'Analyse et l'Implantation des Solides.

nitrogen (^{14}N and ^{15}N) doses as a function of the incident fluence, which is defined as the number of nitrogen incident atoms. The values were obtained by integrating all the RNRA depth profiles of the implanted species. At fluences lower than 5.5×10^{17} N/cm^2, the retained dose increases linearly with a coefficient close to 1. The saturation is reached for each isotope at a fluence of $\sim 6.0 \times 10^{17}$ N/cm^2, confirming that a given amount of the implanted nitrogen has not been retained in the silicon lattice. It is worth mentioning that both the ion range and the straggle (Table 1) strongly increase with fluences around $\sim 5.0 \times 10^{16}$ N/cm^2 to reach 119.5 nm and 71.7 nm at the high fluence of 1.06×10^{18} N/cm^2, respectively. Kilner et al. [24] reported the formation of N gas bubbles for ion fluences larger than 1.4×10^{18} cm^{-2} (200 keV) that corresponds to an ion fluence of $\sim 6.0 \times 10^{17}$ cm^{-2} for an energy of 30 keV/atom. Thus, the N concentration saturation would correspond to the beginning of N gas bubble formation. The release of gas trapped in these bubbles [33] could explain the fluctuation in the retained dose observed for fluences larger than 6.0×10^{17} cm^{-2}.

The saturation of the nitrogen retained dose could be explained by three different processes. First, the backscattering of ions by the silicon matrix has been calculated by SRIM [26] simulation and is very low (~1.4%). Secondly, the sputtering of the target should be taken into account for the two species contained in the target. At first, incident nitrogen ions sputter only silicon, but implanted nitrogen is also rapidly sputtered. On the opposite, swelling will contribute to increase the nitrogen retention, especially at high fluences, in increasing the implantation layer thickness. Using the results of SRIM simulation and a reasonable swelling, one can calculate that backscattering and sputtering alone cannot explain a saturation of the retained N doses for fluences larger than 6.0×10^{17} cm^{-2}, although these two phenomena could explain that the retained dose increases with a coefficient slightly lower than 1. Nevertheless, SRIM is a static code and this evolution does not appear in the calculations. Thus, another process influences the nitrogen retention. This process could be the thermal diffusion and desorption during the implantation. The diffusion would be strongly enhanced when the local saturation concentration is reached. If it is the case, no isotopic effect can be easily observed. Indeed, with the precision of our measurements, we cannot conclude that an isotopic effect influences the depth profile of ^{14}N and ^{15}N implanted in silicon. Same properties have already been observed for nitrogen implantation into iron [29].

RNRA nitrogen depth profiles of 60 keV $^{14}N_2^+$ and $^{15}N_2^+$ ion implanted silicon at a fluence of 10.6×10^{17} N$^+$/cm^2 at 400 °C are shown in Fig. 3. The ^{14}N (Fig. 3(a)) and ^{15}N (Fig. 3(b)) saturated profiles were measured through $^{14}N(\alpha,\gamma)^{18}F$ at 1.531 MeV and $^{15}N(p,\alpha\gamma)^{12}C$ at 0.429 MeV resonant nuclear reactions, respectively. In both cases, a saturation in the nitrogen distribution with a concentration reaching ~60 at.% has been obtained. A retained ion dose of $\sim 6.0 \times 10^{17}$ N$^+$/cm^2 has been measured in both cases. The broad spreading of the saturated profiles is due to thermal diffusion effects, which usually occur from high-dose implantations at elevated temperature [34]. We can note that 6.0×10^{17} N$^+$/cm^2 corresponds to the values used with gaseous targets for nuclear astrophysics cross sections measurements. Finally, the reproducibility of the nitrogen depth profiles has also been observed on two samples implanted in the same conditions.

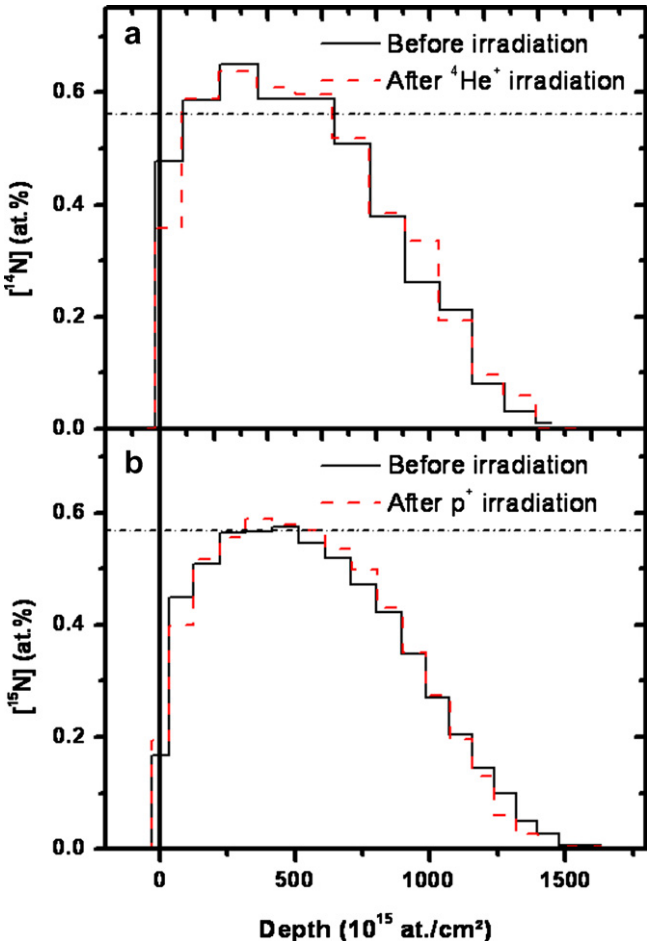

Fig. 3. Comparison of the depth profiles obtained by RNRA before (solid line) and after (dash line) irradiation for the nitrogen (^{14}N (a) and ^{15}N (b)) standards implanted with 1.06×10^{18} N/cm^2 at 30 keV/atom and 400 °C. The irradiations consisted in ion fluences of 3.36×10^{16} $^4He^+$/cm^2 for ^{14}N (a) and 8.60×10^{17} $^1H^+$/cm^2 for ^{15}N (b). The nitrogen concentration in Si_3N_4 compounds is shown.

The composition and structural properties must be controlled in order to ensure a reliable standard. The stability of the ^{14}N standard under 200 nA beam current of 1.546 MeV $^4He^+$ ions and the ^{15}N standard under 250 nA beam current of 0.435 MeV $^1H^+$ ions may be observed in Fig. 4. The number of detected gamma rays, normalized to one nanoCoulomb of incoming ions, gives the evolution of the nitrogen concentration for different irradiating ion fluences. It appears that with irradiation fluence up to $\sim 3.36 \times 10^{16}$ ^4He/cm^2 and to $\sim 8.60 \times 10^{17}$ ^1H/cm^2, the implanted nitrogen profiles remain unchanged. The evolution of the nitrogen desorption can be fitted with a straight

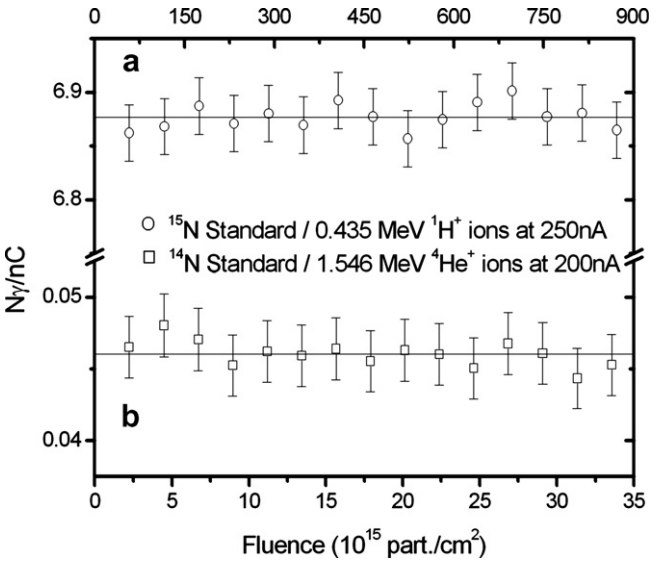

Fig. 4. Ion desorption stability of implanted nitrogen during irradiation of the ^{15}N standard with $^{1}H^{+}$ ions at 0.435 MeV (a) and the ^{14}N standard with $^{4}He^{+}$ ions at 1.546 MeV (b).

line with zero-slope, which means that the implanted nitrogen is stable for the above mentioned ion fluence irradiation. Consequently, the samples obtained can be considered as nitrogen standards.

4. Conclusions

The fabrication of reliable isotopic nitrogen standards has been achieved in $^{14}N_2^+$ and $^{15}N_2^+$ ion implanted Si at 400 °C to a fluence of 10.6×10^{17} N/cm^2. The RNRA and stability data indicate the formation of standards with a high degree of reproducibility. The composition of the implanted Si layers is not affected under ion irradiation suggesting that the stability is maintained. No isotopic effect (^{14}N versus ^{15}N) has been observed, which is in agreement with the fact that thermal diffusion and desorption during the implantation should contribute to the saturation of N retained dose at large ion fluences. The results demonstrate the possibility of using ion implantation in the fabrication of isotopic nitrogen standards, furthering the potential for precise measurements of nuclear cross sections, in particular, for reactions with astrophysical interest involving both nitrogen isotopes (^{14}N and ^{15}N). Indeed, the nitrogen standards obtained in this work present the typical number of atoms used with gaseous target in those cross section measurements.

Acknowledgements

The authors thank Gilles Abel for technical help and ion implantation processing. This work has been supported by the SC-TEC02 collaboration between the Wallonie-Bruxelles Community and the government of Québec. M. Yedji is partially supported by the Natural Science and Engineering Research Council of Canada (NSERC). G. Genard was supported as research fellow by the Belgian National Fund for Scientific Research (F.R.S.-FNRS).

References

[1] R. Gibnala, R.F. Hehemann (Eds.), Hydrogen Embrittlement and Stress Corrosion Cracking, ASM-6344, 1984, 324pp.
[2] M. Bruel, Nucl. Instr. and Meth. B 108 (1996) 313.
[3] C. Maleville, B. Aspar, T. Poumeyrol, H. Moriceau, M. Bruel, A.J. Auberton-Herve, T. Barget, Mat. Sci. Eng. B 46 (1997) 14.
[4] X.Q. Feng, Y. Huang, Int. J. Solids Struct. 41 (2004) 4299.
[5] M. Xu, X.Q. Feng, Theor. Appl. Fract. Mech. 42 (2004) 295.
[6] Y.Q. Wang, R. Smirani, G.G. Ross, Physica E 27 (2004) 97.
[7] G. Genard, M. Yedji, G.G. Ross, G. Terwagne, Nucl. Instr. and Meth. B 264 (2007) 156.
[8] C. Silien, I. Marenne, J. Auerhammer, N. Tagmatarchis, K. Prassides, P.A. Thiry, P. Rudolf, Surf. Sci. 482–485 (2001) 1.
[9] T. Maiyalagan, B. Viswanathan, U.V. Varadaraju, Electrochem. Commun. 7 (2005) 905.
[10] G. Terwagne, D.D. Cohen, G.A. Colling, Nucl. Instr. and Meth. B 84 (1994) 415.
[11] H.A. Bethe, Phys. Rev. 55 (1939) 103.
[12] W.A.S. Lamb, R.E. Hester, Phys. Rev. 108 (1957) 1304.
[13] A. Formicola et al., Phys. Lett. B 591 (2004) 61.
[14] R.C. Runkle, A.E. Champagne, C. Angulo, C. Fox, C. Iliadis, R. Longland, J. Pollanen, Phys. Rev. Lett. 94 (2005) 082503.
[15] A. Lemut et al., Phys. Lett. B 634 (2006) 483.
[16] H. Huang, K.J. Winchester, A. Suvorova, B.R. Lawn, Y. Liu, X.Z. Hu, J.M. Dell, L. Faraone, Mater. Sci. Eng. A-Struct. 435 (2006) 453.
[17] B. Reynes, J.C. Bruyère, Sens. Actuatator A-Phys. 32 (1992) 303.
[18] C.D. Meekison, G.R. Booker, K.J. Reeson, L.F. Hemment, R.F. Peart, R.J. Chater, J.A. Kilner, J.R. Davis, J. Appl. Phys. 69 (6) (1991) 3503.
[19] J. Petruzello, T.F. McGee, M.H. Frommer, V. Rumennik, P.A. Walters, C.J. Chou, J. Appl. Phys. 58 (12) (1985) 4605.
[20] Y. Miyagawa, K. Baba, R. Hatada, S. Naka, M. Ikeyama, S. Miyagawa, in: Proceedings of the 1998 International Conference on Ion Implantation Technology, Vol. 2, 1999, p. 1133.
[21] W. Skorupa, K. Wollschlager, U. Kreissig, R. Groetzschel, H. Bartsch, Nucl. Instr. and Meth. B 19/20 (1987) 285.
[22] P. Bourguet, J.M. Dupart, E. Le Tiran, P. Auvray, A. Giuvarc'h, M. Salvi, G. Pelous, P. Henoc, J. Appl. Phys. 51 (1980) 6169.
[23] P.L.F. Hemment, R.F. Peart, M.F. Yao, K.G. Stephens, R.J. Chater, J.A. Kilner, D. Meekison, G.R. Booker, R.P. Arrowsmith, Appl. Phys. Lett. 46 (1985) 952.
[24] J.A. Kilner, R.J. Chater, P.L.F. Hemment, R.F. Peart, K.J. Reeson, R.P. Arrowsmith, J.R. Davis, Nucl. Instr. and Meth. B 15 (1986) 214.
[25] A. Markwitz, H. Baumann, W. Grill, E.F. Krimmel, K. Bethge, Appl. Phys. Lett. 64 (1994) 2652.
[26] J.P. Biersack, J.F. Ziegler, SRIM-2000, <http://www.research.ibm.com>.
[27] C.R. Gossett, Nucl. Instr. and Meth. B 10/11 (1985) 722.
[28] B. Maurel, G. Amsel, Nucl. Instr. and Meth. 218 (1983) 159.
[29] G. Terwagne, M. Piette, F. Bodart, Nucl. Instr. and Meth. B 19 (1987) 145.
[30] K.M. Horn, W.A. Lanford, Nucl. Instr. and Meth. B 34 (1988) 1.
[31] G. Terwagne, S. Lucas, F. Bodart, Nucl. Instr. and Meth. B 66 (1992) 262.
[32] J.R. Tesmer, M. Nastasi (Eds.), Handbook of Modern Ion Beam Materials Analysis, MRS, Pittsburg, 1995.
[33] B. Terreault, G. Ross, R.G. St-Jacques, G. Veilleux, J. Appl. Phys. 51 (3) (1980) 1491.
[34] M. Piette, G. Terwagne, W. Möller, F. Bodart, Mater. Sci. Eng. B-Solid 2 (1989) 189.